EFFECT OF LEAD CONTENT ON THE FORMATION OF THE 2223 PHASE*

M. Lelovic, P. Krishnaraj, N. G. Eror, W. A. Soffa, and V. L. Richards
Dept. of Materials Science and Engineering
University of Pittsburgh
Pittsburgh, PA

U. Balachandran
Energy Technology Division
Argonne National Laboratory
Argonne, IL

June 1993

Submitted to *Physica C.*

*Work supported by the U.S. Department of Energy, Energy Efficiency and Renewable Energy, as part of a program to develop electric power technology, under Contract W-31-109-Eng-38.

Effect of lead content on the formation of the 2223 phase in the Bi-Sr-Ca-Cu-O system

M.Lelovic, P.Krishnaraj, N.G.Eror, W.A.Soffa, V.L.Richards
(Dept. of Materials Science and Eng., University of Pittsburgh)

U.Balachandran
(~~Materials and Components~~ Energy Technology Division,
Argonne National Laboratory, Argonne IL)

Abstract:

Freeze-dried powders have been used for the formation of the high Tc (110 K) superconducting phase in the Bi-Sr-Ca-Cu-O system. Effects of lead content and oxygen partial pressure were investigated. It was shown that lead content and oxygen partial pressure were affecting liquid phase formation. Lead content affected the dissolution of the 2212 phase into the liquid phase from which the 2223 high Tc superconducting phase forms. Powder reacted as pellet with $Bi_{1.8}Pb_{0.4}Sr_{2.0}Ca_{2.0}Cu_{3.0}O_x$ composition shows essentially phase pure 2223 after 12 hrs at 845° C in 7%O_2.

1.Introduction

In the last couple of years, significant effort has been made towards synthesing of high Tc (110 K) single phase $Bi_2Sr_2Ca_2Cu_3O_x$ (2223), in the Bi-Sr-Ca-Cu-O system. Due to the limited transport of different cations, it is difficult to produce high volume fractions of this phase by conventional solid-state processing.

A brief overview on points that will be considered in the present paper includes: effect of lead content on liquid phase formation, effect of oxygen partial pressure on liquid phase formation and the actual formation mechanism of the high Tc 2223 phase. It is well known that partial substitution of lead for bismuth has a stabilizing effect on the 2223 phase[1-4]. However, the exact role of the lead ions and the nature of the stabilization is not clear. One approach considers lead ions as a liquid phase former via the decomposition of Ca_2PbO_4[5,6]. Idemoto et al.,[5] studied annealing effects on the lead - doped superconductor at various temperatures and oxygen pressures. Ca_2PbO_4 was shown to form over a significant range of PO_2. Another way of looking at the effect is to consider lead ions as a bismuth substitute, i.e. lead is only present in Bi-containing phases. A systematic study of 21 compositions on a compositional line connecting all three superconducting phases was done in the temperature range of 825° C - 1100° C in static air[7]. The reported observation was that no specific lead-

containing phase was detected (Ca_2PbO_4 or Sr_2PbO_4), and lead was only present in bismuth-containing phases. Hong and Mason [8] studied solid-solution ranges in the $Bi_2Sr_2CaCu_2O_x$ (2212) and 2223 superconducting phases at 800° C in air. They found the Ca_2PbO_4 phase present in most of the lead doped samples. Both arguments seem to agree with Idemoto's plot.

The importance of the presence of Ca_2PbO_4 in the system has been carefully studied at Argonne National Laboratory [9,10]. A two step powder-in-tube process has produced a Jc as high as 50,000 A/cm^2 at 77 K in zero applied field. In this process, lead-doped 2212 was mixed with Ca_2PbO_4, Ca_2CuO_3 and CuO. DTA results indicated involvment of the Ca_2PbO_4 phase in the formation of a liquid phase during heat treatment. The lead content in the 2212 phase was shown to be an important factor. The highest Ic and Jc values were obtained when all of the Pb was incorporated into 2212 phase.

The effect of oxygen partial pressure on the onset of liquid phase formation in $Bi_{1.8}Pb_{0.4}Sr_{2.0}Ca_{2.2}Cu_{3.0}O_y$ system was demonstrated in our previous report [11]. As the oxygen partial pressure was decreased, the initial temperature for liquid phase formation was also decreased. This behavior correlates with the previous report that the formation of the 2223 phase is promoted by synthesis at reduced oxygen partial pressure [12,13].

The actual formation mechanism of the high Tc phase has not yet been established due to the lack of an appropriate phase diagram. Chen and Stevens [14] used a high resolution electron microscopy to study the formation mechanism of the 2223 phase. They concluded that the actual mechanism is

a three step process: dissolution of the 2212 phase into the liquid phase (liquid phase was formed from the decomposition of Ca_2PbO_4), precipitation of the $Bi_2Sr_2CuO_x$ (2201) phase from the liquid, and (nucleation and) growth of the 2223 phase from the 2201 phase. The final state was a mixture of the 2223 phase and a 2201 grain boundary phase. Different results were reported by Umezawa et al.[15] showing the presence of the 2212 phase at grain boundaries. Even in the sample showing only x-ray diffraction peaks for the 2223 phase, one unit cell of the 2212 phase was present at the grain boundary.

In this paper, we report on the relationship between lead content, oxygen partial pressure, and microstructure of the superconducting phases. Lead content and oxygen partial pressure was shown to affect the formation of the liquid phase. The lead content in the 2212 phase affected its dissolution into the liquid phase from which the 2223 high Tc phase forms.

2.Experimental Procedure

Samples used in this study were prepared by a freeze-drying process , as described previously[11]. Advantages of the freeze-drying process over conventional solid-state methods for $YBa_2Cu_3O_y$ and $(Bi,Pb)_2Sr_2Ca_2Cu_3O_y$ have been described elsewhere[16,17,18].

Powders were mixed with three compositions: $Bi_{2.0}Sr_{2.0}Ca_{2.0}Cu_{3.0}Oy$, $Bi_{1.8}Pb_{0.2}Sr_{2.0}Ca_{2.0}Cu_{3.0}O_y$, and $Bi_{1.8}Pb_{0.4}Sr_{2.0}Ca_{2.0}Cu_{3.0}O_y$. After freezing nitrate solutions of each composition, drying was done in two steps; the first drying was carried out in a commercial freeze-dryer (Edwards High Vacuum, Supermoduluo 45) from -40° C to 20° C, and the second drying in an oven up to 125 °C at a slow rate of 5° C/hr. The green colored powder was then heated in a controled atmosphere furnace at 650 °C for 1hr. Denitrated powders were then ground, pressed into pellets and heat treated at 845 °C in a 7%O_2-Argon atmosphere.

Differential thermal analysis (DTA) and thermogravimetric analysis (TGA) were used to characterize the dehydration and denitration steps. Heat treated samples were characterized by X-ray diffractometry (XRD) using CuKα radiation. Morphology and compositional analysis were performed using scanning transmission electron microscopy (STEM).

3. Results

A) TGA and DTA analysis

Figure 1 a shows combined TGA and DTA runs for a $Bi_{1.8}Pb_{0.4}Sr_{2.0}Ca_{2.0}Cu_{3.0}O_x$ composition with a heating rate of 5° C / min in a 7% O_2 - Argon atmosphere. The TGA curve showed a weight loss of ~ 2% for heating up to 200° C that corresponded to the removal of water. The denitritation process occurs between 200° C and 550° C. The scale of the TGA run is enlarged between 600° C and 900° C in Fig.1b. The onset of liquid phase formation was associated with a change in slope at ~ 790° C. Between 830° C and 860° C, the TGA curve does not show any transformation due to the slow transformation kinetics as compared to the heating rate of the TGA.

Since we are able to detect the initiation of liquid phase formation, a plot was constructed of onset temperature for liquid phase - vs - lead content at different oxygen partial pressures (Figure 2). An increase in lead content and decrease in oxygen partial pressure decreased the initiation temperature by ~40° C.

B) XRD analysis

Figure 3 shows the XRD pattern for a sample without lead sintered for [1] 2 hrs; [2] 2+5 hrs; and [3] 2+5+5 hrs at 845° C in 7%O_2. Each step is accompanied by grinding and pelletizing. After 7 hrs, the 2212 phase becomes stable with no indication of the 2223 high Tc phase peaks. Low angle peaks shown in the inset indicate only the (002) peak for the 2212 phase (m) was present.

In a specimen with the composition $Bi_{1.8}Pb_{0.2}Sr_{2.0}Ca_{2.0}Cu_{3.0}O_x$, a small volume fraction of the 2223 high Tc phase is detected after 7 hrs (Figure 4) shown by the diffraction peak at 2θ equal 4.7 ° corresponding to the (002) plane for the 2223 high Tc phase. The 2212 phase was the major phase after 12 hrs as can be seen for from curve [3].

Figure 5 shows the XRD pattern for a sample with the composition $Bi_{1.8}Pb_{0.4}Sr_{2.0}Ca_{2.0}Cu_{3.0}O_x$. After an initial 2 hrs at 845° C, 2212 appeared as the major phase; however, after 7 hrs, peaks characteristic of the 2223 high Tc phase appeared (2θ equal 26.3° for (115) plane of the 2223 high Tc phase) accompanied by disappearance of peaks characteristic of the 2212 phase. After an additional 5 hrs at 845° C (total time of 12 hrs), the high Tc phase was the main phase and only a small volume fraction of 2201 phase was detected. The peak at 2θ equals 7.3 ° is characteristic of the (002) plane of the 2201 phase.

C) STEM analysis

Microsructural analysis was carried out for the various heat treatments for the XRD samples for the $Bi_{1.8}Pb_{0.4}Sr_{2.0}Ca_{2.0}Cu_{3.0}O_x$ composition. Figure 6 a is a high resolution TEM micrograph taken in the dark field (DF) image mode for a sample heat treated for 2 hrs at 845° C (XRD pattern [1] in Figure 5) showing the coexistance of a crystalline phase (A) and an amorphous phase (B). From the diffraction patterns and spacing between lattice fringes of ~3.0nm, the crystalline phase was established to be 2212. The diffraction pattern from the amorphous phase is shown in the insert. The X-ray spectra from energy dispersive spectroscopy (EDS) was performed on both grains as shown in Figure 6 b. It was observed that both regions have chemical compositions close to the 2212 stoichiometric ratio.

Figure 7 a is a TEM micrograph taken in a bright field (BF) image mode for a sample heat treated for 7 hrs at 845° C (XRD pattern [2] in Figure 5). Three grains are shown with the grain boundaries indicated by arrows. A microbeam diffraction pattern (MBD) from grain C is presented in Figure 7 b. The grain labeled D is shown to be an amorphous (the MBD is shown in Figure 7c). A selected area diffraction (SAD) pattern from the large grain labeled E is shown in Figure 7 d. A simulated diffraction pattern created by the diffraction software "DIFRACT" version 1.3n is shown in Figure 7 (e). EDS analysis from all regions is shown in Figure 7 f. As can be observed, regions

C and E have similar compositions close to the 2223 stoichiometric ratio. The amorphous region between two grains exhibits peaks for all the constitutive cations. A qualitative comparison of the relative ratios of the L-peaks of Bi and Cu for the amorphous (D) and crystalline (C,E) regions indicates that the amorphous region contains less Cu than the surrounding crystalline regions

4.Discussion

In our previous report[11] the synthesis of the $Bi_{1.8}Pb_{0.4}Sr_{2.0}Ca_{2.2}Cu_{3.0}O_x$ composition by a freeze drying process was emphasized. A splat cooling step has been adopted to overcome the limitations of low freezing rates and subsequent segregation of precursors. A two step drying procedure has been applied for the removal of waters of hydration.

The onset temperature for liquid phase formation can be lowered with the addition of lead and/or a decrease in oxygen partial pressure. The weight loss associated with the formation of the liquid phase can be detected using TGA with a heating rate of 5° C/min. As shown in Figure 2 a, decrease in oxygen partial pressure for the sample without lead lowers the initial temperature by ~ 20° C. The interpretation of weight loss results are complicated by other concurrent effects such as the exchange of oxygen between the sample and environment, variation in the oxygen content and oxygen diffusion in the 2212 system (without lead) [19,20]. If the reported[20] Arrhenius-type behavior for the diffusion of oxygen into the lead free 2212 phase is used, a diffusivity of $D \sim 4\ 10^{-5}$ (cm^2/s) is obtained at 800° C. This indicates that the weight loss measured by TGA,in a sample without lead, is actually a difference between oxygen gain by the 2212 phase and oxygen loss due to the formation of the liquid phase. An increase in lead content up to

0.4 lowers the onset temperature for the formation of liquid phase from 810 °C to 790 °C (7%O2 atmosphere). This fact seems to favour arguments about Ca_2PbO_4 phase formation and, therefore, the role of lead as a liquid phase former.

An increase in lead content not only affected the formation of the liquid phase but also affected the formation and stabilization of the high Tc 2223 phase. From the XRD data for the sample with a $Bi_{1.8}Pb_{0.4}Sr_{2.0}Ca_{2.0}Cu_{3.0}O_x$ composition, a significant amount of 2223 phase has been detected after heat treating for 7 hrs at 845° C (Figure 5, curve[2]) . However, XRD data for the sample without lead for the same heat treatment (Figure 3, curve [2]), shows the 2212 phase as the major phase with no indication of peaks characteristic of the 2223 high Tc phase. This experimental observation indicates that the lead content actually affected the dissolution of the 2212 phase into the liquid phase. If the lead content in the initial composition becomes greater than ~20% of the Bi content then the 2212 phase will dissolve. If the ratio of bismuth to lead is smaller than 20% , the 2212 phase will not dissolve completely (Figure 4, curve [2]) and will remain even upon further heat treatments.

To verify observations from TGA, DTA and XRD measurements, high resolution microscopy coupled with EDS analysis was performed. As shown in Figure 6 a, the coexistance of the 2212 phase and amorphous phase was verified. The MBD diffraction pattern from the amorphous phase exhibited only one diffuse ring. The dissolution interface lies along the c-plane

indicating that the dissolution process occurs preferentially along a and b planes due to the short diffusion paths. EDS analysis from both regions showed presence of lead and bismuth (Figure 6 b). This was at least a qualitative indication that the presence of lead in a certain amount in the 2212 phase was affecting its dissolution behavior. The presented observation correlates well with the study at ANL[9]. The highest Ic and Jc values were obtained when all of the lead was incorporated into 2212 phase.

Figure 7 shows the formation of the high Tc 2223 phase from the liquid phase. C and E are 2223 grains and D is the amorphous phase between them. EDS analysis shows a smaller amount of Cu with respect to Bi for the amorphous phase. The presence of lead with bismuth in the amorphous phase was evident.

This observation is in general agreement with the report by Chen and Stevens[14]. The actual formation mechanism of the 2223 high Tc phase consists of the dissolution of the 2212 phase into the liquid phase and subsequent nucleation and growth of the high Tc phase out of the liquid phase. Particles of 2201 phase have been found inside the grains of the 2223 high Tc phase[11].

The possible applications for powders with the $Bi_{1.8}Pb_{0.4}Sr_{2.0}Ca_{2.0}Cu_{3.0}O_x$ composition for wire processing employing a powder-in-tube process is currently being investigated.

Conclusions:

The onset temperature for liquid phase formation in Bi-Sr-Ca-Cu-O system was lowered by both lead doping and a decrease in oxygen partial pressure. The increase in lead content also increased the rate of formation and increased the stability of the 2223 phase. If the lead concentration was less than ~ 20 % of the bismuth content, the 2212 phase did not dissolve completely.

High resolution TEM demonstrated that the 2212 phase dissolves along the a and b planes. The 2223 phase then grows from the liquid phase by nucleation and growth.

Acknowledgements:

We would like to thank Mr C. Van Ormer for his help with the microscopy.

This work is supported by the U.S.Department of Energy (DOE), Conservation and Renewable Energy, as part of a DOE program to develop electric power technology under contract W-31-109-Eng-38.

Figures

Fig. 1a : DTA and TGA of dehydrated powder of $Bi_{1.8}Pb_{0.4}Sr_{2.0}Ca_{2.0}Cu_{3.0}O_x$ composition, shows complete removal of nitrates after 600° C

Fig. 1b : Detail of TGA scan of the same sample as 1 a, exhibits onset of liquid phase formation

Fig. 2 : The onset temperature for liquid phase formation as a function of lead content and oxygen-partial pressure

A: 7 % O_2; B: 21 % O_2

Fig.3 : XRD of the sample $Bi_{2.0}Sr_{2.0}Ca_{2.0}Cu_{3.0}O_x$, sintered at 845 °C in 7%O_2-atmosphere, showing stabilization of the 2212 phase. Each step represents grinding and pelletizing. Shown in inset is the detail of the low angle peak, (002) reflection, for the 2212 phase.

[1] : 2 hr; [2] : 2+5 hrs; [3] : 2+5+5 hrs

Fig. 4 : XRD of the sample $Bi_{1.8}Pb_{0.2}Sr_{2.0}Ca_{2.0}Cu_{3.0}O_x$, sintered at 845° C in 7%O_2-atmosphere, showing the presence of 2212 as

the major phase, and the 2223 phase. Shown in inset is the detail of the low angle peaks, (002) reflection, for the 2212 and 2223 phases.

[1] : 2 hr; [2] : 2+5 hrs; [3] : 2+5+5 hrs

Fig.5 : XRD of the sample $Bi_{1.8}Pb_{0.4}Sr_{2.0}Ca_{2.0}Cu_{3.0}O_x$, sintered at 845° C in 7%O_2-atmosphere, showing the progression of 2223 phase formation. Also, in inset is the detail of low angle peaks, (002) reflection, for the 2223 and 2201 phases.
[1] : 2 hr; [2] : 2+5 hrs; [3] : 2+5+5 hrs

Fig.6 : TEM micrographs of the sample $Bi_{1.8}Pb_{0.4}Sr_{2.0}Ca_{2.0}Cu_{3.0}O_x$ after sintering for 2 hrs at 845° C in 7%O_2.

a) High resolution DF image showing coexistance of the 2212 phase (grain A) and amorphous phase (grain B). Shown in inset is the MBD diffraction pattern from the amorphous region.

b) X-ray spectra from the grain A and from the grain B

Fig.7 : TEM micrographs of the sample $Bi_{1.8}Pb_{0.4}Sr_{2.0}Ca_{2.0}Cu_{3.0}O_x$ after 2+5 hrs at 845 °C in 7%O_2 atmosphere

a) BF image showing three grains; grain boundaries are indicated with arrows

b) MBD diffraction pattern from the grain (C) ; (711) zone axis for 2223 phase

c) MBD diffraction pattern showing amorphous nature for grain (D)

d) SAD diffraction pattern from grain (E); (711) zone axis for 2223 phase

e) Simulated diffraction pattern showing indexed spots for (711) zone axis for 2223 phase

f) X-ray spectra from the grains (C), (D) and (E)

References:

1) S.A.Sunshine, T.Siegrist, L.F.Shneemeyer, D.W.Murphy, R.J.Cava, B.Batlogg, R.B. van Dover, R.M.Fleming, S.H. Glarum, S.Nakahara, R.Farrow, J.J. Krajewski, S.M. Zahurak, J.W. Wasczak, J.P.Marshall, P. Marsh, L.W. Rupp, and W.F.Peck, Phys.Rev.B. Condens.Mater.,38 [1] (1988) 893

2) R.J.Cava, B.Batlogg, S.A.Sunshine, T.Siegrist, R.M.Fleming, K.Rabe, L.F.Schneemeyer, D.W.Murphy, R.B.van Dover, P.K.Gallagher, S.H.Glarum, S.Nakahara, R.C.Farrow, J.J.Krajewski, S.M.Zahurak, J.V.Waszczak, J.H.Marshall, P.Marsh, L.W.Rupp Jr., W.F.Peck and E.A.Rietman , Physica C 153-155 (1988) 560-565

3) B.W.Statt, Z.Wang, M.J.G.Lee, J.V.Yakhmi, P.C.De Camargo, J.F.Major and J.W.Rutter, Physica C 156 (1988) 251-255

4) U.Balachandran, D.Shi, D.I.Dos Santos, S.W.Graham, M.A.Patel, B.Tani, K.Vandervoort, H.Claus and R.B.Poeppel, Physica C 156 (1988) 649-651

5) Y.Idemoto, S.Ichikawa and K.Fueki, Physica C 181 (1991) 171-178

6) M.Xie, L.W.Zhang, T.G.Chen, X.T.Li and J.Cai, Physica C 206 (1993) 251-253

7) P.Strobel, J.C.Toledano, D.Morin, J.Schneck, G.Vacquier, O.Monnereau, J.Primot and T.Fournier, Physica C 201 (1992) 27-42

8) B.Hong and T.O.Mason, J.Amer.Cer.Soc., 74 [5] 1045-52 (1991)

9) Practical Superconductor Development for Electrical Power Applications, Argonne National Lab., Monthly Technical Status Report - Feb. 1993

10) U.Balachandran, private communication

11) P.Krishnaraj, M.Lelovic, N.G.Eror and U.Balachandran, Physica C, submitted

12) U.Endo, S.Koyama and T.Kawai, Jpn.J.Appl.Phys. 27 (1988) L1476

13) U.Endo, S.Koyama and T.Kawai, Jpn.J.Appl.Phys. 27 (1988)

L1861

14) V.L.Chen and R.Stevens, J.Amer.Cer.Soc. 75 [5] 1992 (1142)

15) A.Umezawa, Y.Feng, H.Edelman, Y.High, D.Larbalestier, Y.Sung and S.Flasher , Physica C 198 (1992) 261

16) M.Strasik and N.G.Eror, " A Novel Preparation Technique for High Temperature Superconductor YBa2Cu3Oy " , Proceedings of MRS

Symposium on Atomic and Molecular Processing of Electronic and Ceramic Materials, (Sept. 1987), 189

17) K.H.Song, H.Liu, S.Dou and C.C.Sorrell, J.Amer.Cer.Soc. 73 [6] 1990 (1771-73)

18) V.Primo, F.Sapina, M.J.Sanchis, R.Ibaniz, A.Beltran and D.Beltran, Materials Letters 15 (1992) 149-155

19) G.Triscone, J.Y.Genoud, T.Graf, A.Junod and J.Muller, Physica C 176 (1991) 247-256

20) S.McKernan and A.Zettl, Physica C 209 (1993) 585-590

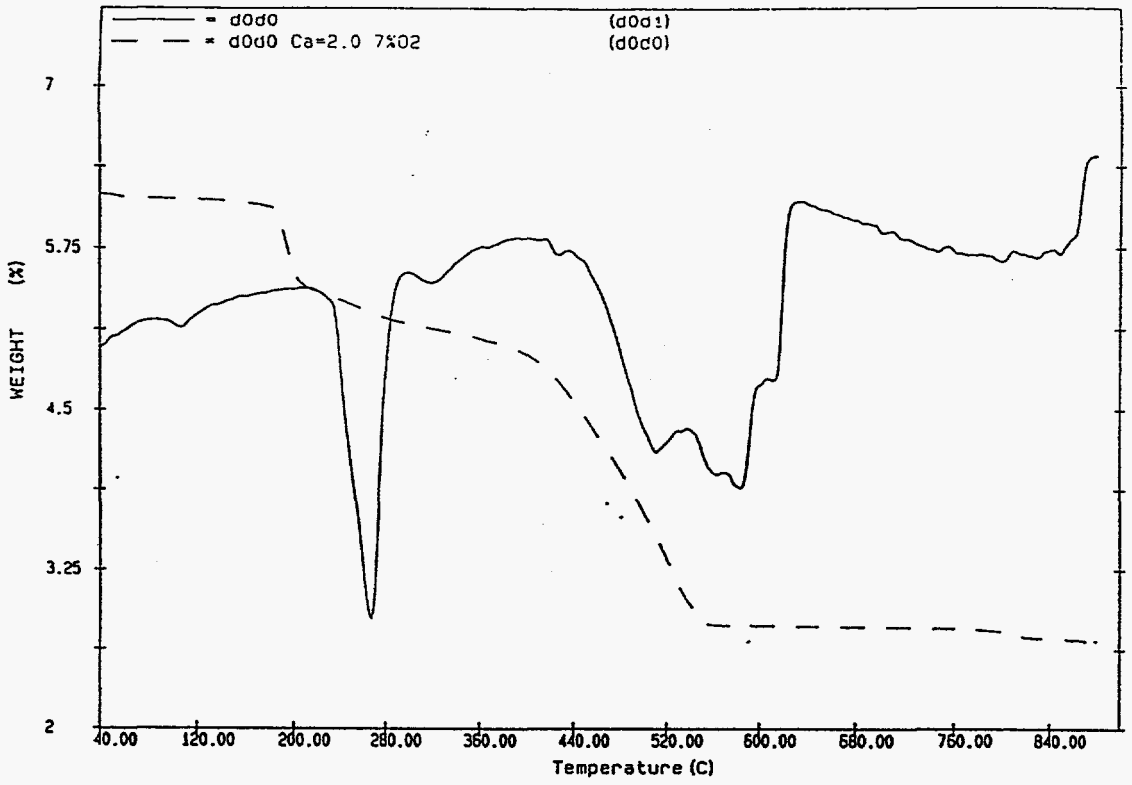
d0d0 (d0d1)
d0d0 Ca=2.0 7%02 (d0d0)
7
5.75
4.5
3.25
2
WEIGHT (%)
40.00
120.00
200.00
280.00
360.00
440.00
520.00
600.00
680.00
760.00
840.00
Temperature (C)

FIGURE 1a

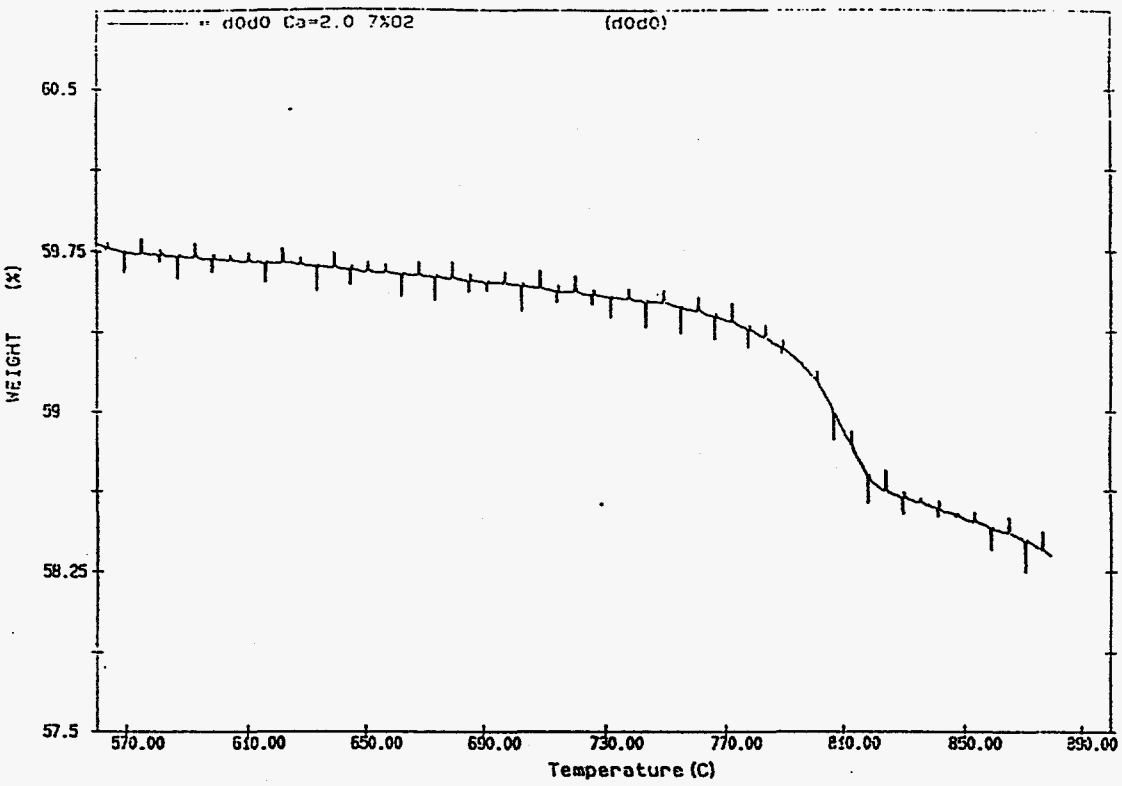
d0d0 Ca=2.0 7%02
(d0d0)
60.5
59.75
59
58.25
57.5
WEIGHT (%)
570.00
610.00
650.00
690.00
730.00
770.00
810.00
850.00
890.00
Temperature (C)

FIGURE 16

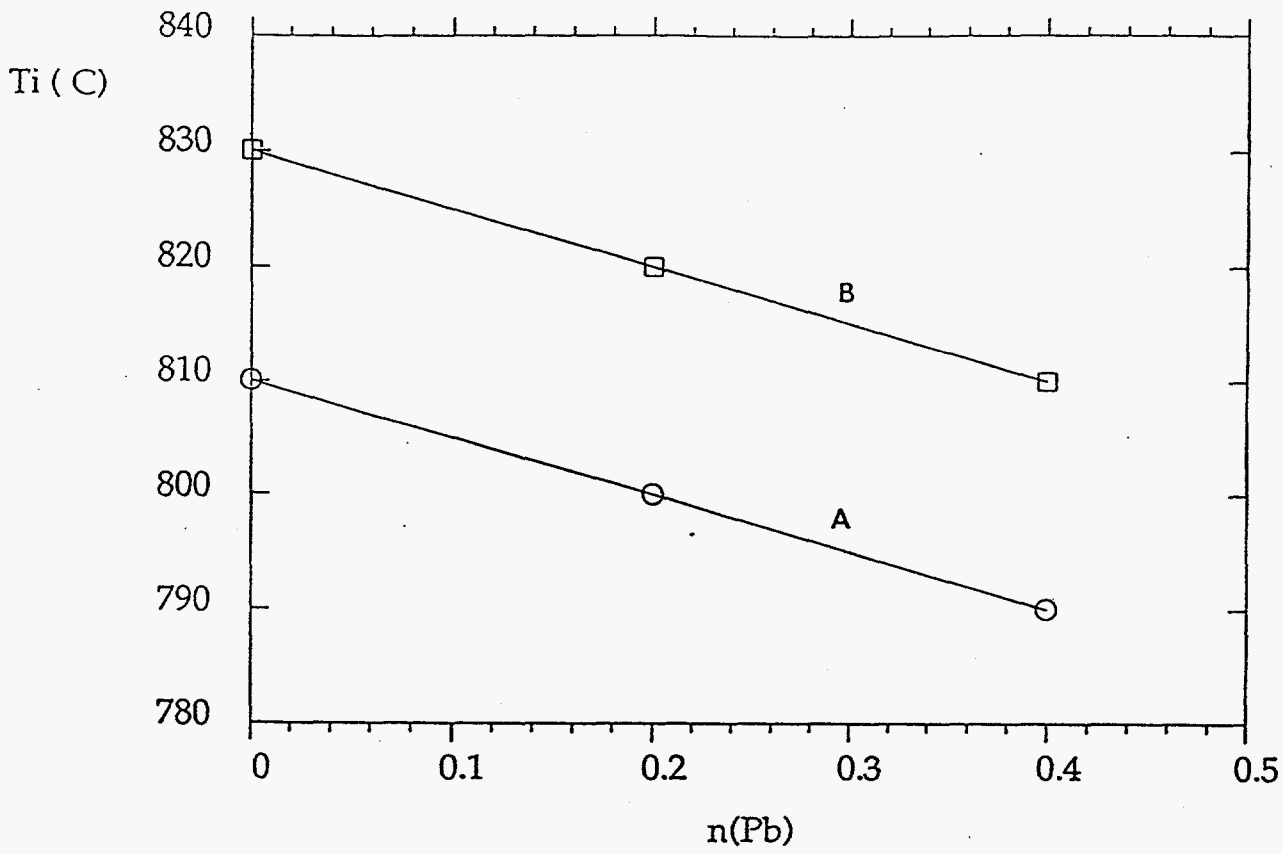

FIGURE 2

A: 7 % O_2 - ARGON

B: 21 % O_2 - ARGON

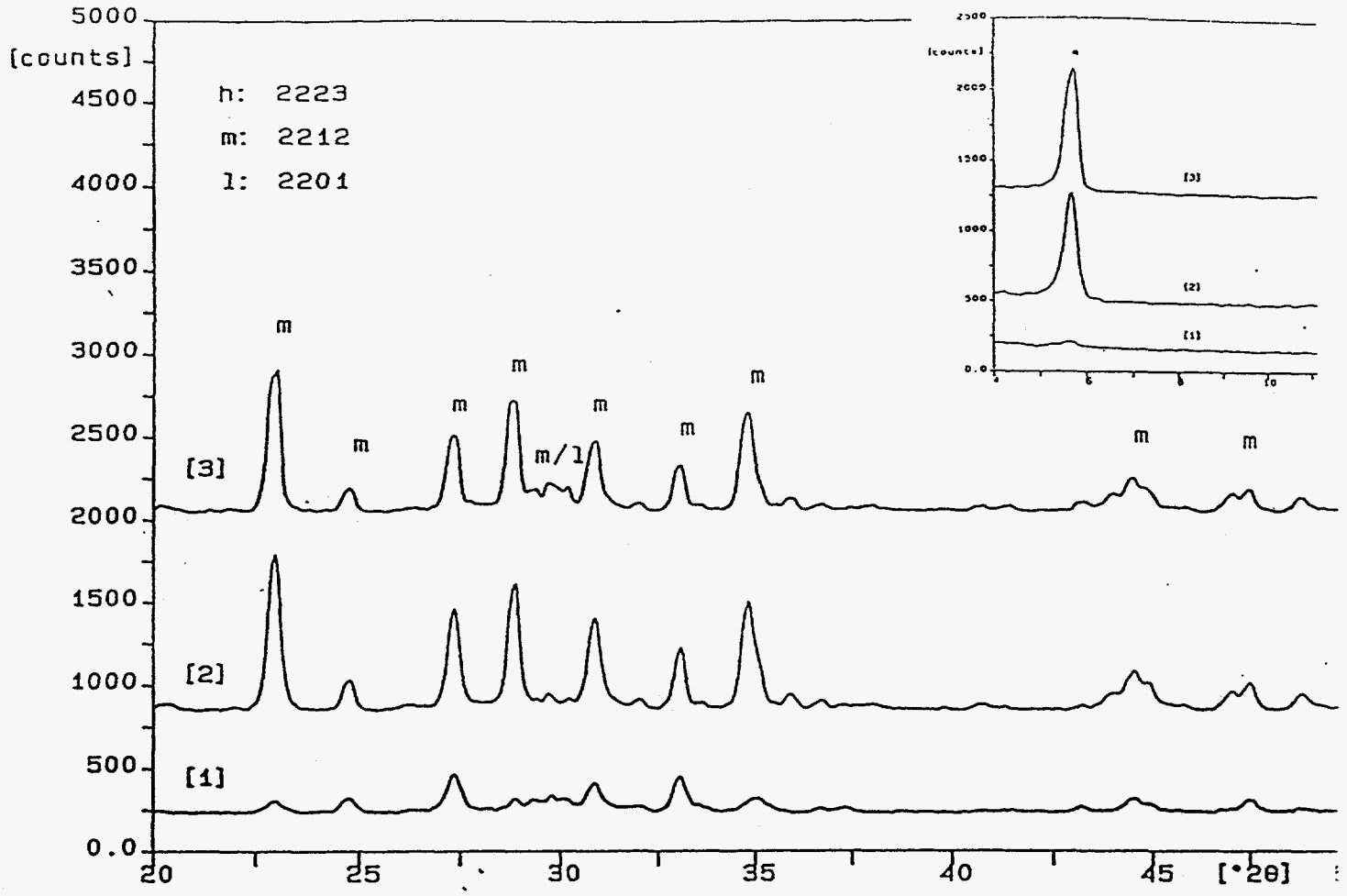
5000
[counts]
4500
4000
3500
3000
2500
2000
1500
1000
500
0.0
h: 2223
m: 2212
l: 2201
[3]
[2]
[1]
m
m/l
20
25
30
35
40
45
[°2θ]

FIGURE 3

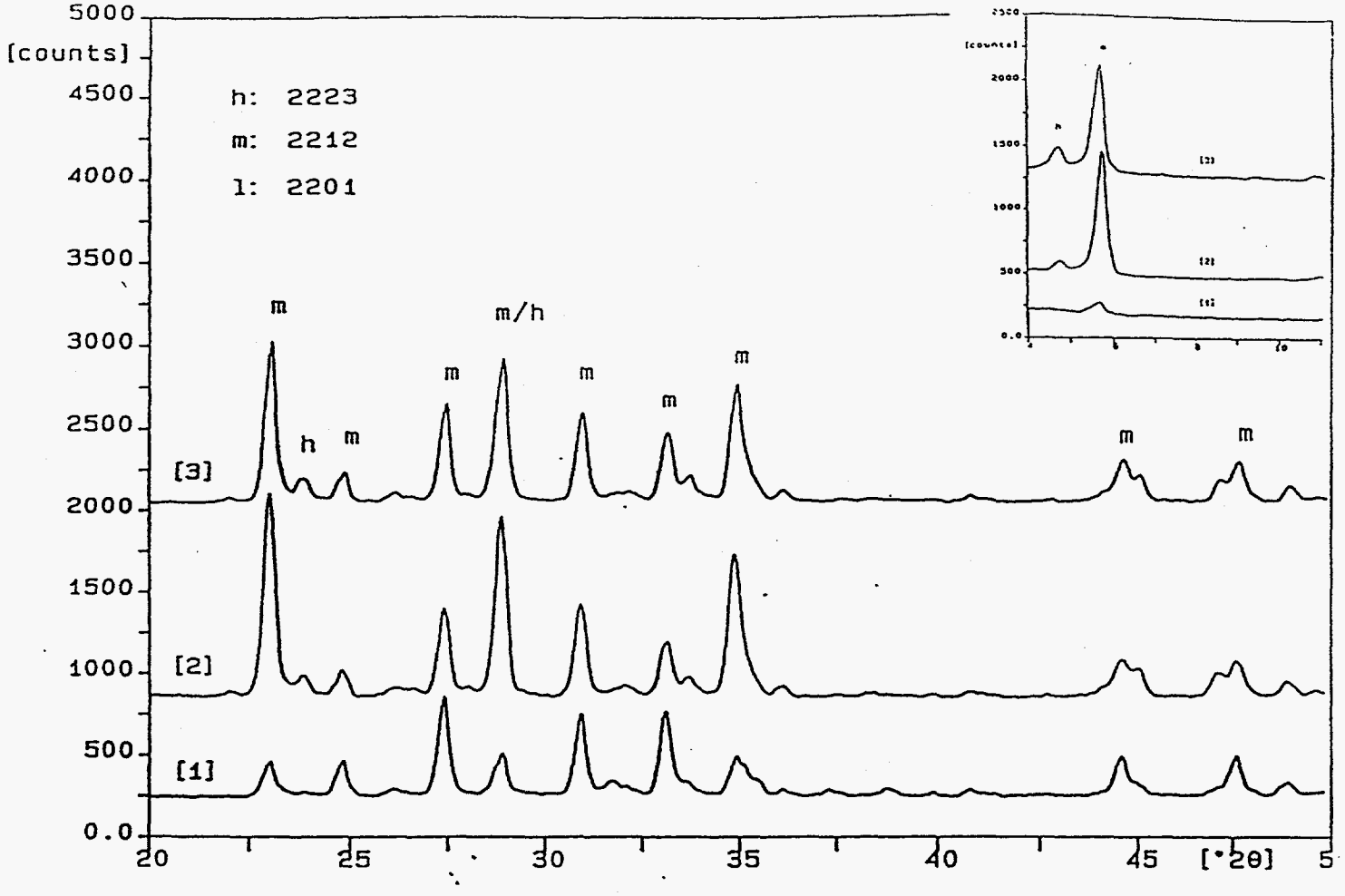
5000
[counts]
4500
4000
3500
3000
2500
2000
1500
1000
500
0.0
h: 2223
m: 2212
l: 2201
m
h
m
m
m/h
m
m
m
m
m
[3]
[2]
[1]
20
25
30
35
40
45
[°2θ]
5

FIGURE 4

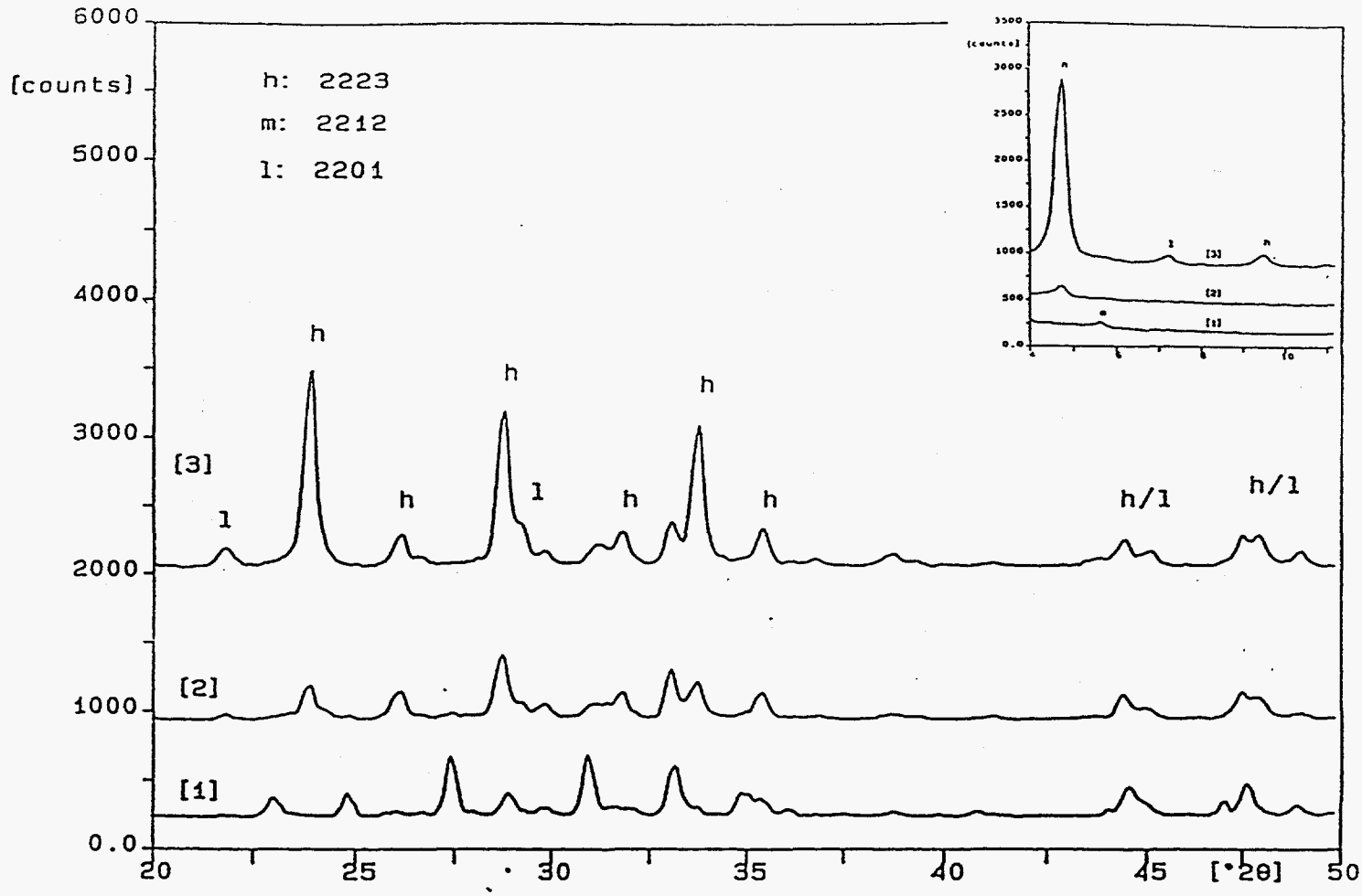
6000
[counts]
5000
4000
3000
2000
1000
0.0
h: 2223
m: 2212
l: 2201
[3]
[2]
[1]
l
h
h
l
h
h
h/l
h/l
20
25
30
35
40
45
[°2θ]
50

FIGURE 5

845°C / 24 hr / 17% O2

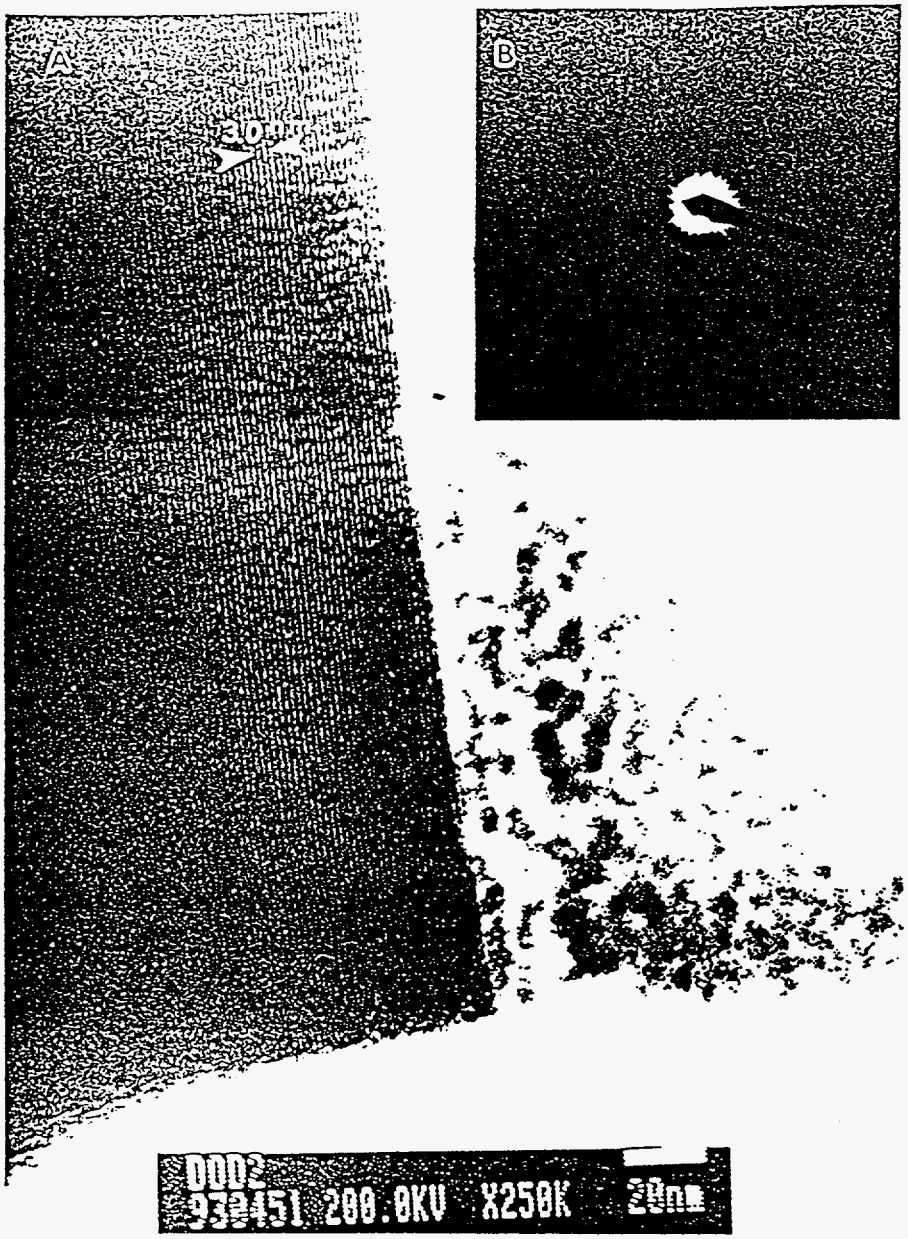

FIGURE 6 a

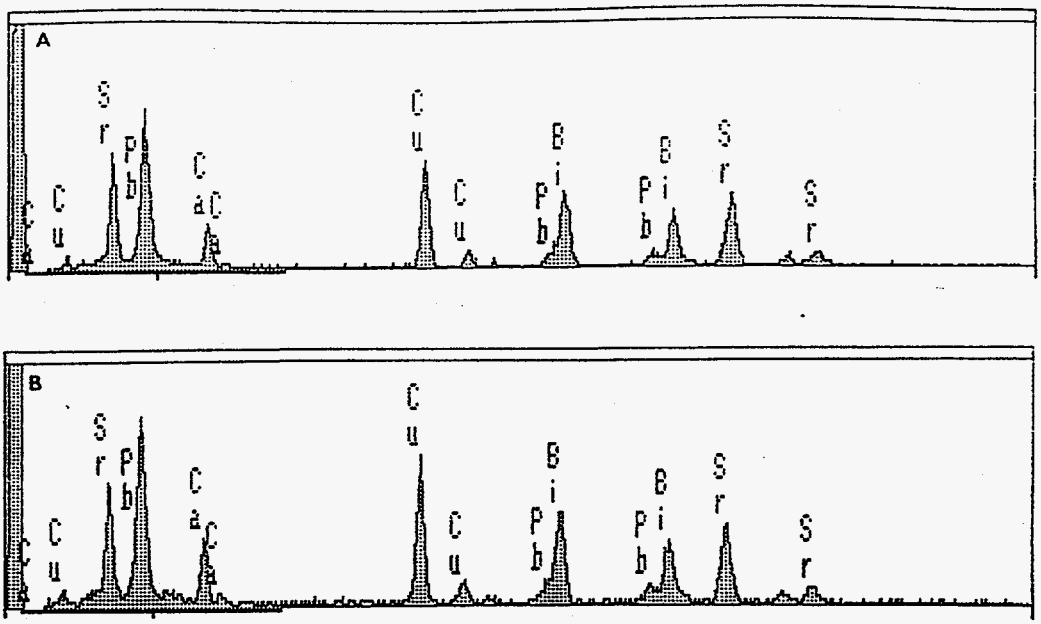
A
Sr
Pb
Cu
Ca
Cu
Cu
Bi
Pb
Bi
Pb
Sr
Sr
B
Sr
Pb
Cu
Ca
Cu
Cu
Bi
Pb
Bi
Pb
Sr
Sr

FIGURE 6 b

FIGURE 7 a

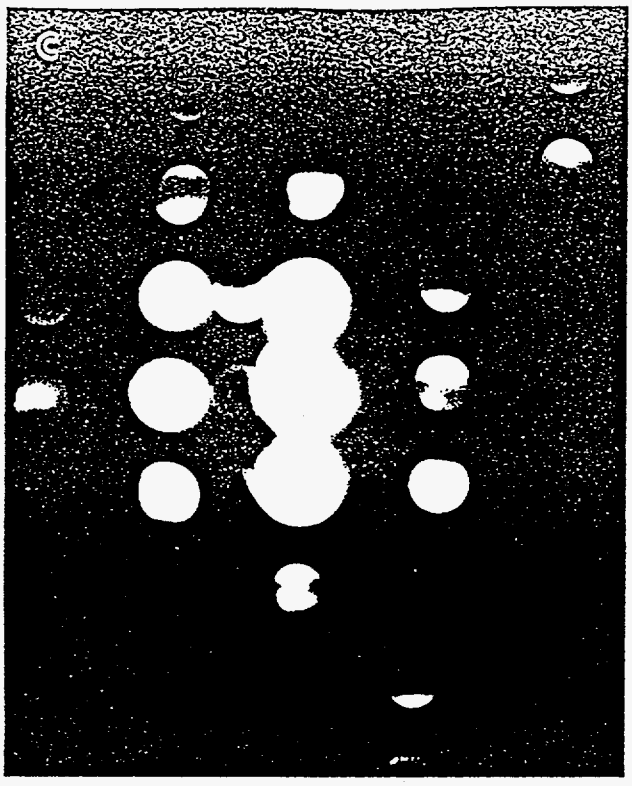

FIGURE 7 6

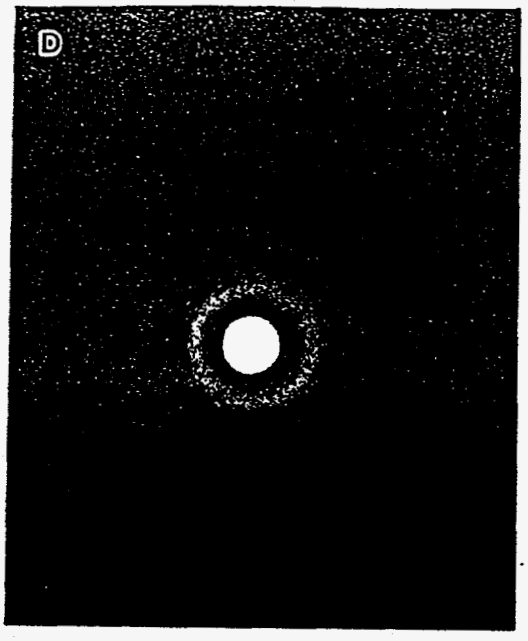

FIGURE 7 C

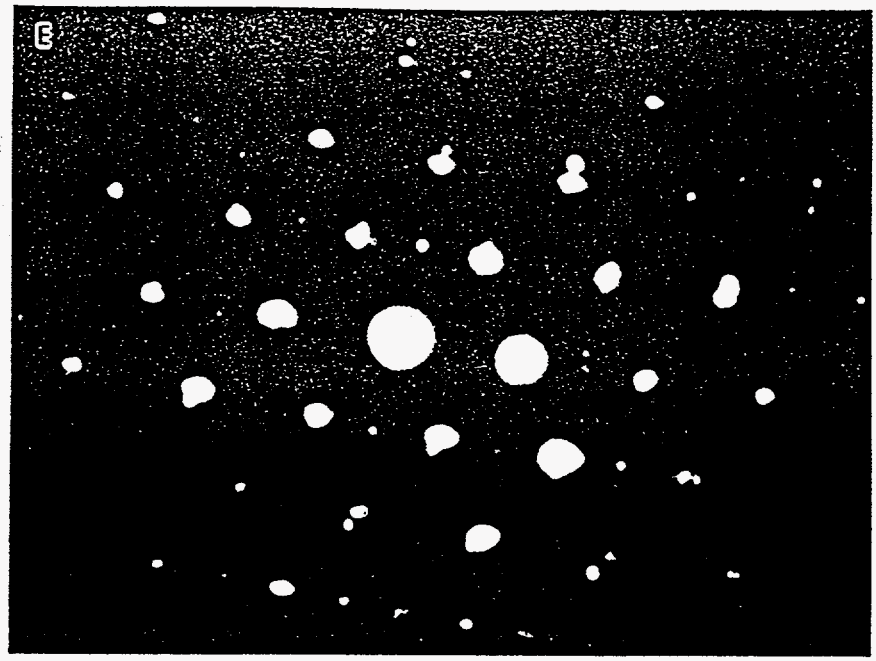

FIGURE 7 d

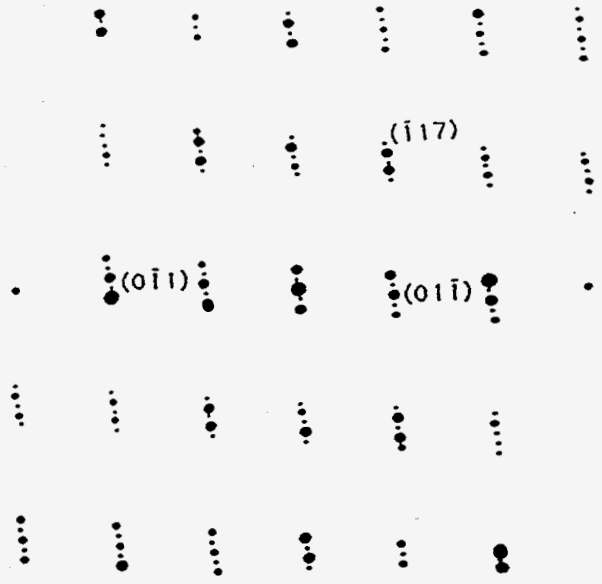

<711> za 2223

FIGURE 7 e

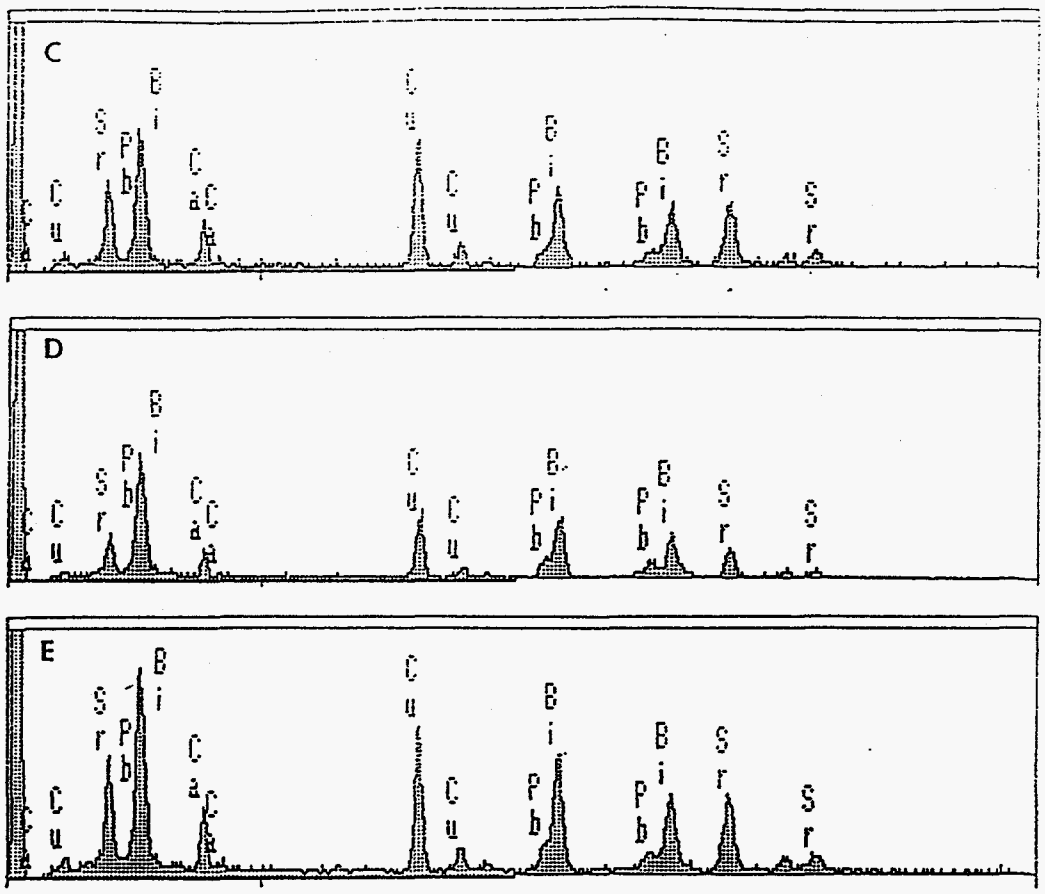

FIGURE 7 f